Current Research in Physiology 5 (2022) 232–239

Contents lists available at ScienceDirect

Current Research in Physiology

journal homepage: www.sciencedirect.com/journal/current-research-in-physiology

Empagliflozin restores cardiac metabolic flexibility in diet-induced obese C57BL6/J mice

Bingxian Xie [a,1], Wesley Ramirez [a,1], Amanda M. Mills [a], Brydie R. Huckestein [a], Moira Anderson [a], Martha M. Pangburn [a], Eric Y. Lang [a], Steven J. Mullet [b,c], Byron W. Chuan [d], Lanping Guo [d], Ian Sipula [a], Christopher P. O'Donnell [d], Stacy G. Wendell [b,c], Iain Scott [e,f,**,1], Michael J. Jurczak [a,f,*,2]

[a] Division of Endocrinology and Metabolism, Department of Medicine, University of Pittsburgh, Pittsburgh, PA, USA
[b] Department of Pharmacology and Chemical Biology, University of Pittsburgh, Pittsburgh, PA, USA
[c] Health Sciences Metabolomics and Lipidomics Core, University of Pittsburgh, Pittsburgh, PA, USA
[d] Division of Pulmonary, Allergy and Critical Care Medicine, Department of Medicine, University of Pittsburgh, Pittsburgh, PA, USA
[e] Division of Cardiology, Department of Medicine, University of Pittsburgh, Pittsburgh, PA, USA
[f] Center for Metabolism and Mitochondrial Medicine, University of Pittsburgh, Pittsburgh, PA, USA

A B S T R A C T

Sodium-glucose co-transporter type 2 (SGLT2) inhibitor therapy to treat type 2 diabetes unexpectedly reduced all-cause mortality and hospitalization due to heart failure in several large-scale clinical trials, and has since been shown to produce similar cardiovascular disease-protective effects in patients without diabetes. How SGLT2 inhibitor therapy improves cardiovascular disease outcomes remains incompletely understood. Metabolic flexibility refers to the ability of a cell or organ to adjust its use of metabolic substrates, such as glucose or fatty acids, in response to physiological or pathophysiological conditions, and is a feature of a healthy heart that may be lost during diabetic cardiomyopathy and in the failing heart. We therefore undertook studies to determine the effects of SGLT2 inhibitor therapy on cardiac metabolic flexibility *in vivo* in obese, insulin resistant mice using a [$U^{13}C$]-glucose infusion during fasting and hyperinsulinemic euglycemic clamp. Relative rates of cardiac glucose versus fatty acid use during fasting were unaffected by EMPA, whereas insulin-stimulated rates of glucose use were significantly increased by EMPA, alongside significant improvements in cardiac insulin signaling. These metabolic effects of EMPA were associated with reduced cardiac hypertrophy and protection from ischemia. These observations suggest that the cardiovascular disease-protective effects of SGLT2 inhibitors may in part be explained by beneficial effects on cardiac metabolic substrate selection.

1. Introduction

Inhibition of the sodium-glucose co-transporter type 2 (SGLT2) has received growing acceptance as a novel, safe, and effective means to improve glycemic control in patients with type 2 diabetes. SGLT2 is a symport transport protein found primarily in the proximal tubule of the kidney where it is responsible for the majority of glucose reabsorption (Vallon et al., 2011). Thus, inhibition of SGLT2 lowers the renal glucose threshold and reduces blood glucose levels by promoting glycosuria. Unexpectedly, SGLT2 inhibitor therapy is also beneficial for patients with cardiovascular disease (CVD). Results from EMPA-REG OUTCOME, a clinical trial to establish the effects of the SGLT2 inhibitor empagliflozin (EMPA) on CVD outcomes in patients with type 2 diabetes at high risk of CVD, demonstrated marked reductions in mortality and rates of hospitalization due to heart failure in patients taking EMPA compared with placebo (Zinman et al., 2015). More recent large-scale clinical trials evaluating CVD-related outcomes of the SGLT2 inhibitors canagliflozin (CANVAS) (Neal et al., 2017) and dapagliflozin (DECLARE-TIMI 58) (Wiviott et al., 2019) produced similar findings, demonstrating that the effects on mortality and heart failure hospitalizations are a class effect and not specific to one inhibitor. Furthermore, clinical trials designed to evaluate the cardio-protective effects of SGLT2 inhibitor therapy across a breadth of heart failure phenotypes, including heart failure with reduced (DAPA-HF, EMPEROR-Reduced) or preserved

* Corresponding author. Department of Medicine University of Pittsburgh 200 Lothrop Street, BST W1060 Pittsburgh, PA, 15213, USA.
** Corresponding author. Department of Medicine University of Pittsburgh, 200 Lothrop Street, BST E1259, Pittsburgh, PA, 15213, USA.
E-mail addresses: iain.scott@pitt.edu (I. Scott), jurczakm@pitt.edu (M.J. Jurczak).
[1] Denotes co-first authors.
[2] Denotes co-senior authors.

https://doi.org/10.1016/j.crphys.2022.05.003
Received 14 January 2022; Received in revised form 29 April 2022; Accepted 17 May 2022
Available online 28 May 2022

(EMPEROR-Preserved) ejection fraction and acute heart failure (EMPULSE) have all shown a consistent benefit (McMurray et al., 2019; Packer et al., 2020; Anker et al., 2021; Voors et al., 2022). While the preponderance of evidence demonstrates a clear beneficial effect of SGLT2 inhibitor therapy on CVD-related outcomes, the underlying mechanism(s) for these observed benefits remain unclear.

A large number of putative mechanisms for the CVD protective effects of SGLT2 inhibitors are proposed and are the topic of recent reviews (Lopaschuk Gary and Verma, 2020; Lam Carolyn et al., 2019; Perry and Shulman, 2020). Several proposed mechanisms focus on changes in cardiac metabolism that restore bioenergetic capacity and improve cardiac efficiency, both of which decline during diabetic cardiomyopathy and heart failure (Neubauer, 2007; Jia et al., 2018). Previous studies exploring a metabolic basis for the CVD-protective effects of EMPA relied on static measures of cardiac or plasma metabolites or changes in gene expression, *ex vivo* approaches utilizing isolated cells or perfused working hearts, or *in vivo* measures of trans-cardiac metabolite concentrations (Verma et al., 2018; Shao et al., 2019; Yurista et al., 2019; Santos-Gallego Carlos Requena-Ibanez Juan Antonio San Antonio Rodolfo et al., 2019). In order to understand whether changes in cardiac metabolism in response to EMPA occur *in vivo*, we applied a stable isotope tracing approach in awake mice under physiological conditions, in order to measure cardiac-specific rates of relative glucose and fatty acid oxidation during fasting and in response to hyperinsulinemic-euglycemic clamp.

2. Materials and methods

2.1. Animal care and use

Mice were studied at the University of Pittsburgh according to guidelines established by the Institutional Care and Use Committee. Age-matched male high-fat diet-fed (HFD; Research Diets D12492 60% kcal fat, 5.21 kcal/g) and control low-fat diet-fed (LFD; Research Diets D12450B 10% kcal fat, 3.82 kcal/g) mice were purchased from Jackson Labs (stock 380050 and 380056). Mice were fed custom diets beginning at 6 weeks of age and were studied at 30 weeks old, such that custom diets were fed for 24 weeks where the last four weeks included EMPA (10 $mg \bullet kg^{-1} \bullet day^{-1}$) in the HFD + E group. EMPA dosing was chosen based on previous studies showing CVD benefits at a 10 mg/kg dose for similar duration (Verma et al., 2018; Habibi et al., 2017; N Dimitriadis et al., 2018). Metabolic cage studies consisted of 72h of analysis in the Columbus Labs Comprehensive Lab Animal Monitoring System where n = 4 LFD and n = 6 HFD and HFD + E were studied. For fasting/re-feeding studies, mice were fasted overnight and euthanized at 7am or fasted overnight and re-fed for 1 h prior to euthanasia. Group sizes of n = 6 for fasted and n = 6 re-fed LFD, HFD, and HFD + E mice were compared.

2.2. Biochemical analyses

Urine and plasma glucose levels were measured by the glucose oxidase method using the Analox GM9. Plasma insulin was measured using the Stellux chemiluminescent insulin ELISA. Plasma glucagon levels were measured using ELISA Kit from Millipore. Plasma fatty acid and β-hydroxybutyrate levels were measured spectrophotometrically using commercially available kits from Wako and Sigma.

2.3. Echocardiography

M-mode echocardiography was performed using the Vevo 3100 (Visualsonics) in isofluorane-anesthetized mice and data were analyzed by Vevo LAB software. Group sizes of n = 15 LFD and N = 16 HFD and HFD + E were studied.

2.4. Coronary artery ligations

Mice underwent open thoracotomy to place a suture around the left anterior descending artery and left loose (sham) or tightly tied (coronary artery ligation), as previously described (McGaffin et al., 2011). Briefly, mice were anesthetized, intubated, ventilated and a small incision was made on the left chest through the fourth intercostal space. The pericardium was opened and the left anterior descending coronary artery was tied off at its mid-segment with a suture to induce myocardial infarction. The suture was left intact for seven days after which the mice were euthanized for heart collection and dissection of the infarct, peri-infarct and remote heart regions. Group sizes of n = 3–4 were used for sham studies and n = 5–6 per group were used for CAL studies.

2.5. Gene expression and western blotting

Quantitative PCR and western blotting were performed as previously described (Edmunds et al., 2020). Primers were designed with Primer-s3web (https://primer3.ut.ee/) or purchased from Qiagen. Sequences for designed primers were as follows: Slc2a1(Glut1) (F:5′-TTGTTGTAGAGCGAGCTGGA-3′ R:5′- ATGGCCACGATGCTCAGATA -3′); Slc2a4(Glut4) (F:5′- CTGGGCTTGGAGTCTATGCT-3′ R:5′-CGCTTTAGACTCTTTCGGGC-3′); and Cpt1b (F:5′- GTCGCTTCTTC AAGGTCTGG-3′ R:5′- AAGAAAGCAGCACGTTCGAT-3′). Primary antibodies were as follows: GAPDH (FL-335), Santa Cruz, SC-25778; Akt (pan) (40D4), Cell Signaling, 2920S; p-Akt (pSer473), Cell Signaling, 4060P; PDH (C54G1), Cell Signaling, 3205; p-PDH (Ser293), Cell Signaling, 37115.

2.6. Cardiac-specific substrate utilization

Mice underwent surgery to implant an indwelling catheter in the right jugular vein and recovered five days prior to study. Mice were fasted 6 h in the morning prior to study. To determine cardiac-specific substrate use and metabolic flexibility, mice were infused with [$U^{13}C$]-glucose at a rate of 1 $mg \bullet kg^{-1} \bullet min^{-1}$ for 120 min to achieve steady-state for the fasted state, or underwent a 120 min hyperinsulinemic-euglycemic clamp where [$U^{13}C$]-glucose (25% enriched ^{13}C enriched 20% dextrose) was infused to maintain euglycemia and match plasma glucose levels during the last 40-min of the study, or steady-state. Insulin was given as a primed/continuous infusion (Novolin-R, Novo Nordisk; prime dose: 30 mU/kg over 3 min; continuous dose: 4.5 $mU \bullet kg^{-1} \bullet min^{-1}$). After each study, mice were sacrificed and hearts collected within 15 s of euthanasia and snap frozen in liquid nitrogen. Frozen hearts were pulverized and processed for analysis by liquid chromatography mass spectrometry (LC-MS) to determine enrichments of [1,2,3–^{13}C]-pyruvate and [1,2–^{13}C]-acetyl-CoA for the calculation of carbohydrate flux through pyruvate dehydrogenase (V_{PDH}) relative to total mitochondrial TCA cycle flux (V_{TCA}), or V_{PDH}/V_{TCA}, as previously described (Thapa et al., 2019). The ratio of [1,2–^{13}C]-acetyl-CoA to [1,2,3–^{13}C]-pyruvate reflects V_{PDH} relative to V_{TCA}, such that a ratio of one indicates 100% glucose oxidation and any reduction in this ratio reflects dilution of [1,2–^{13}C]-acetyl-CoA by unlabeled acetyl-CoA from other sources, primarily fatty acid oxidation. Due to difficulties in measuring isotopologues of acetyl-CoA and pyruvate related to pool size in the fasted samples during LC/MS, [4,5–^{13}C]-glutamate and [1,2,3–^{13}C]-lactate were used as surrogates for [1,2–^{13}C]-acetyl-CoA and [1,2,3–^{13}C] pyruvate, respectively, as previously described (Alves et al., 2011; Shulman et al., 1987). Isotopologues of [1,2–^{13}C]-acetyl-CoA and [1,2,3–^{13}C]-lactate were used for calculations in insulin clamped mice. Groups sizes of n = 4 LFD, n = 6 HFD and n = 3 HFD + E were used for fasted studies and n = 5, n = 4 HFD and n = 5 HFD + E were used for hyperinsulinemic studies.

2.7. Statistical analyses

Data shown are the mean ± s.e.m. and were compared by one-way ANOVA followed by Tukey's multiple comparison test or Student's t-test where noted. For all comparisons $p < 0.05$ was considered significant.

3. Results

3.1. EMPA promotes glucosuria and whole-body fat oxidation

Urine glucose concentrations were increased 7- and 5-fold in HFD + E compared with LFD and HFD mice, respectively (Fig. 1A; $P < 0.001$). The respiratory exchange ratio, indicative of relative glucose and fat oxidation, was reduced in HFD compared with LFD mice, demonstrating increased whole-body fat oxidation in the HFD group (Fig. 1B; $P < 0.01$). The respiratory exchange ratio was further reduced in HFD + E mice compared with HFD mice (Fig. 1B; $P < 0.05$) consistent with previous reports in rodents and humans demonstrating that SGLT2 inhibition promotes whole-body fat oxidation (Ferrannini et al., 2014, 2016a). Body weight was significantly increased in HFD and HFD + E compared with LFD mice, and there was no difference in body weight between HFD and HFD + E mice (Fig. 1C), likely due to the relatively low dose (10 $mg \cdot kg^{-1} \cdot day^{-1}$) and short duration (4 weeks) of EMPA treatment (see discussion).

Increased plasma glucagon levels and cardiac ketone utilization are thought to contribute to improved CVD outcomes in patients treated with SGLT2 inhibitor therapy (Ferrannini et al., 2016b). We therefore measured plasma levels of a number of hormonal and metabolic factors after fasting and re-feeding. The fasting/re-feeding paradigm produced increases in plasma glucose and insulin levels (Fig. 1D&F), as well as reductions in fatty acid and ketone levels in LFD mice (Fig. 1E&H), indicative of a successful protocol. Fasting plasma glucose levels were significantly increased in HFD and HFD + E compared with LFD mice and there was no difference between HFD and HFD + E mice (Fig. 1D; $P < 0.01$). There were no differences in plasma glucose levels following

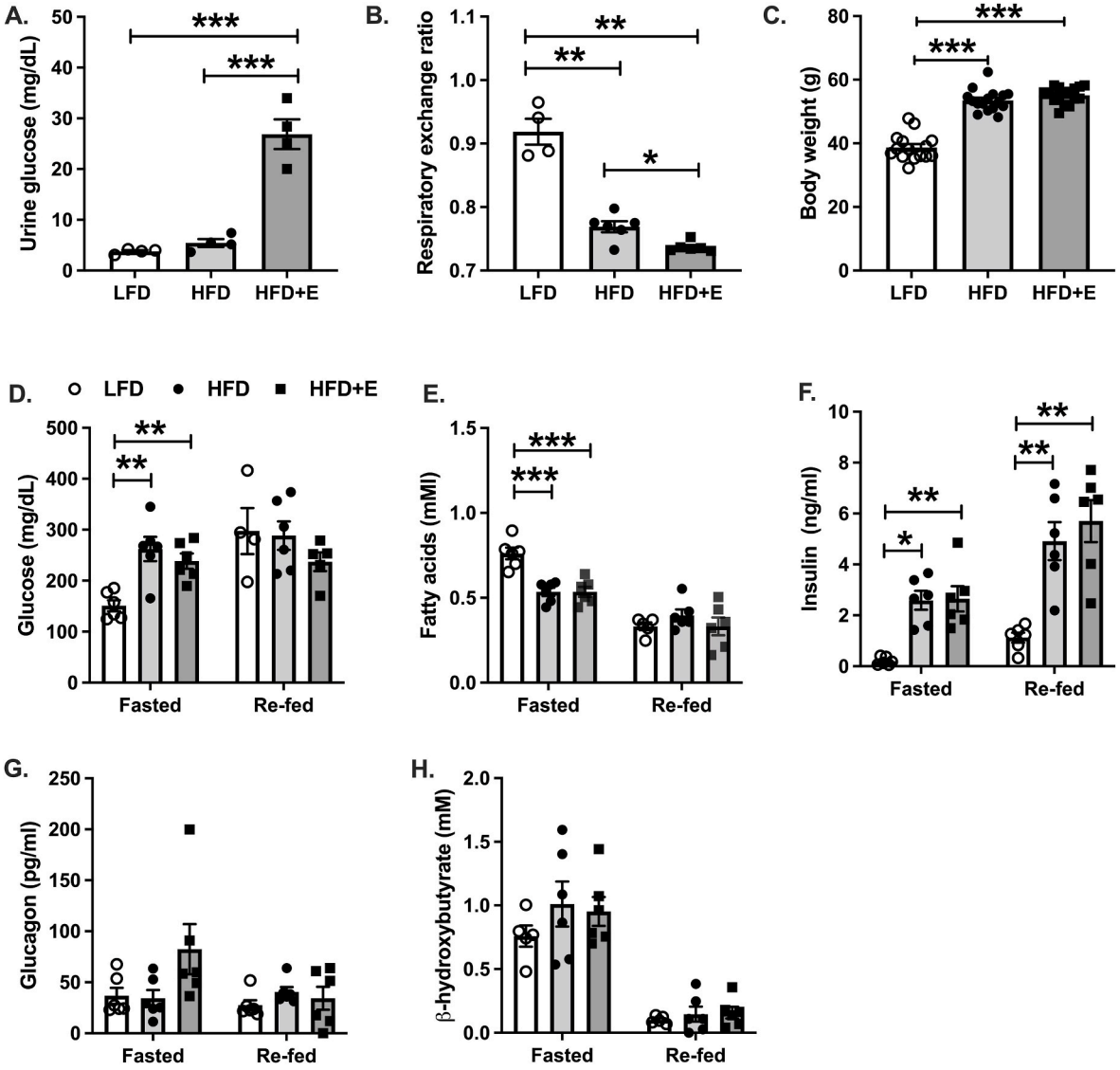

Fig. 1. EMPA increases glucosuria and promotes whole-body lipid oxidation. A. Urine glucose levels measured in the morning in ad libitum fed mice after two weeks of EMPA diet. **B.** The 24h average respiratory exchange ratio measured in metabolic cages during the second week of EMPA treatment. **C.** Body weights after four weeks of EMPA treatment. **D.** Plasma glucose levels by glucose oxidase method. **E.** Plasma fatty acids measured by spectrophotometric assay. **F.** Plasma insulin levels measured by ELISA. **G.** Plasma glucagon levels measured by ELISA. **H.** Plasma β-hydroxybutyrate levels measured by spectrophotometric assay. Data are the mean ± s.e.m. for groups of n = 4–6 for A-B, n = 15–16 for C, and n = 6 for D-H. Data were compared by one-way ANOVA and followed by multiple comparison testing to compare all groups when a significant effect was observed. *$P < 0.05$, **$P < 0.01$, ***$P < 0.001$.

re-feeding between groups (Fig. 1D). Plasma insulin levels were significantly increased in HFD and HFD + E compared with LFD mice in both fasted and re-fed mice, and there were no differences between HFD and HFD + E mice (Fig. 1E). There were no differences in plasma glucagon levels between groups in either the fasted or re-fed states, although plasma glucagon levels in fasted HFD + E mice appeared modestly elevated compared with LFD and HFD mice (Fig. 1G; $P = 0.11$). Fasted plasma fatty acid levels were significantly reduced in HFD and HFD + E mice compared with LFD and there no differences between HFD and HFD + E mice (Fig. 1E; $P < 0.001$). There were no differences in re-fed plasma fatty acid levels between groups (Fig. 1E). Lastly, plasma levels of β-hydroxybutyrate were not different between groups in either the fasted or re-fed state (Fig. 1H).

3.2. Cardiac hypertrophy and susceptibility to ischemic stress are improved in EMPA-treated mice

Next, we assessed ventricular mass and dimensions as surrogates of cardiac hypertrophy using echocardiography in anesthetized mice. During diastole, the interventricular septum width (IVSd) was significantly increased in HFD and HFD + E compared with LFD mice, and reduced in HFD + E compared with HFD mice (Fig. 2A; $P < 0.001$, $P < 0.05$ and $P < 0.05$, respectively). There were no differences in the left ventricle internal dimension (LVID) or the left ventricular posterior wall (LVPW; Fig. 2B&C). During systole, there were no differences in LVID between groups (Fig. 2D). The estimated left ventricular mass (LV mass) was significantly increased in HFD compared with LFD mice, and reduced in HFD + E compared with HFD mice (Fig. 2E; $P < 0.001$ and $P < 0.05$, respectively).

To determine whether EMPA protected against a cardiac-specific stress in our model, we performed coronary artery ligations and sacrificed mice seven days after the procedure in order to isolate the area of infarct, peri-infarct and remote heart. Expression of the cardiac stress-related genes B-type natriuretic peptide (*Bnp*) and atrial natriuretic peptide (*Anp*) appeared elevated in the area of infarct compared with sham treated mice from each group, indicative of a successful procedure (Fig. 2F&G). *Bnp* expression was significantly different in the remote heart (Fig. 2F; $P < 0.05$). Multiple comparison testing did not detect significant differences between groups, although there were trends for increased *Bnp* expression in HFD compared with LFD and HFD + E (Fig. 2F; $P = 0.07$ and $P = 0.06$, respectively). Similar observations were made for *Anp* expression in remote heart, where the effect of group trended towards significance (Fig. 2G; $P = 0.05$), and multiple comparison testing detected similar trends of increased *Anp* expression in HFD compared with LFD and HFD + E (Fig. 2G; $P = 0.07$ and $P = 0.08$, respectively). Expression of *Bnp* and *Anp* in the area of infarct and peri-infarct did not differ between groups, despite a similar pattern of expression as observed in the remote heart (Fig. 2F&G).

3.3. EMPA restores cardiac metabolic flexibility

Cardiac-specific substrate selection was measured after a 6h morning fast or during a hyperinsulinemic euglycemic-clamp by infusing mice with [U^{13}C]-glucose. Plasma glucose levels were matched at approximately 110 mg/dL across all three groups during steady-state, or the last 40 min of the clamp (Fig. 3A upper panel; $P = 0.7$ for average plasma glucose levels during steady-state compared by 1-way ANOVA, data not shown). The average glucose infusion rate (GIR) required to maintain euglycemia during steady-state was significantly greater in LFD compared with HFD and HFD + E, demonstrating impaired whole-body insulin sensitivity in the HFD and HFD + E mice (Fig. 3A lower panel and 3B; $P < 0.001$). There was no difference in whole-body insulin sensitivity between HFD and HFD + E mice (Fig. 3A lower panel and 3B; $P = 0.29$). In the fasted state, there were no differences in V_{PDH}/V_{TCA} between groups and the measured value of approximately 0.2 reflected 20% glucose and 80% fatty acid utilization (Fig. 3C). During

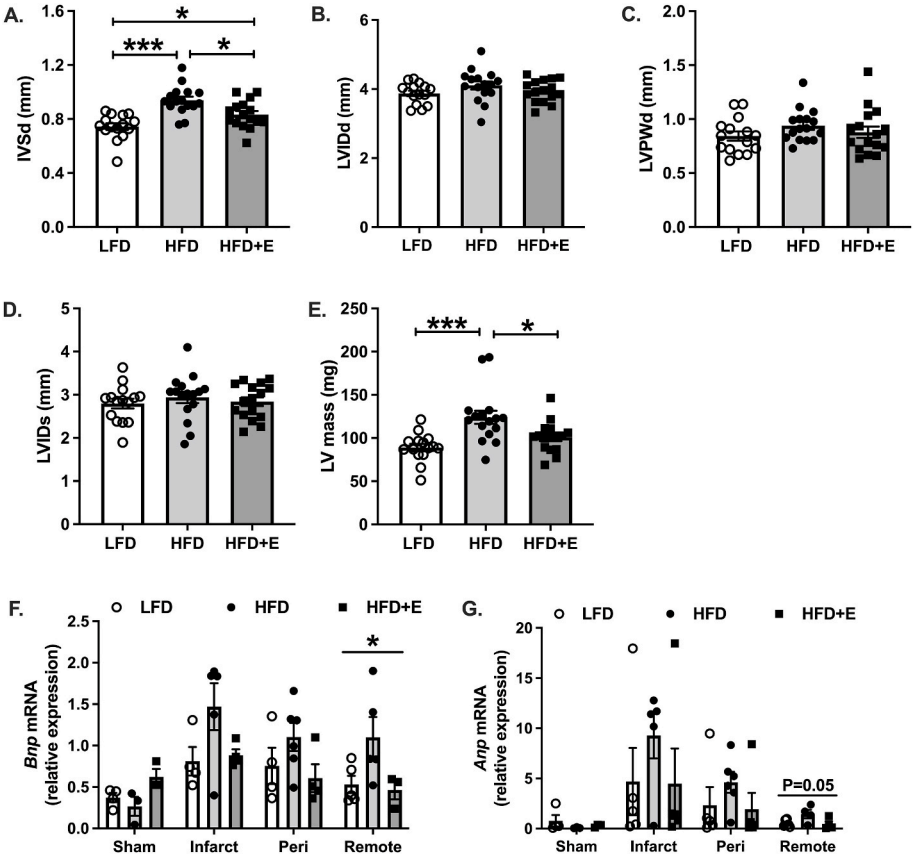

Fig. 2. EMPA-treated micehave reduced cardiac hypertrophy and are protected against ischemia. **A.** Interventricular septum during diastole (IVSd). **B.** Left ventricular internal dimension during diastole (LVIDd). **C.** Left ventricular posterior wall during diastole (LVPWd). **D.** Left ventricular internal dimension during systole (LVIDs). **E.** Estimated left ventricular mass (LV mass). **F-G.** *Bnp* and *Anp* mRNA measured from heart samples of sham operated mice and areas of infarct, peri-infarct and remote heart of mice one week after coronary artery ligations (CAL) without reperfusion. Data are the mean ± s.e.m. for groups of n = 15–16 for A-E and n = 3–4 sham and n = 5–6 for CAL. Data were compared by one-way ANOVA and followed by multiple comparison testing to compare all groups when a significant effect was observed. *$P < 0.05$, ***$P < 0.001$.

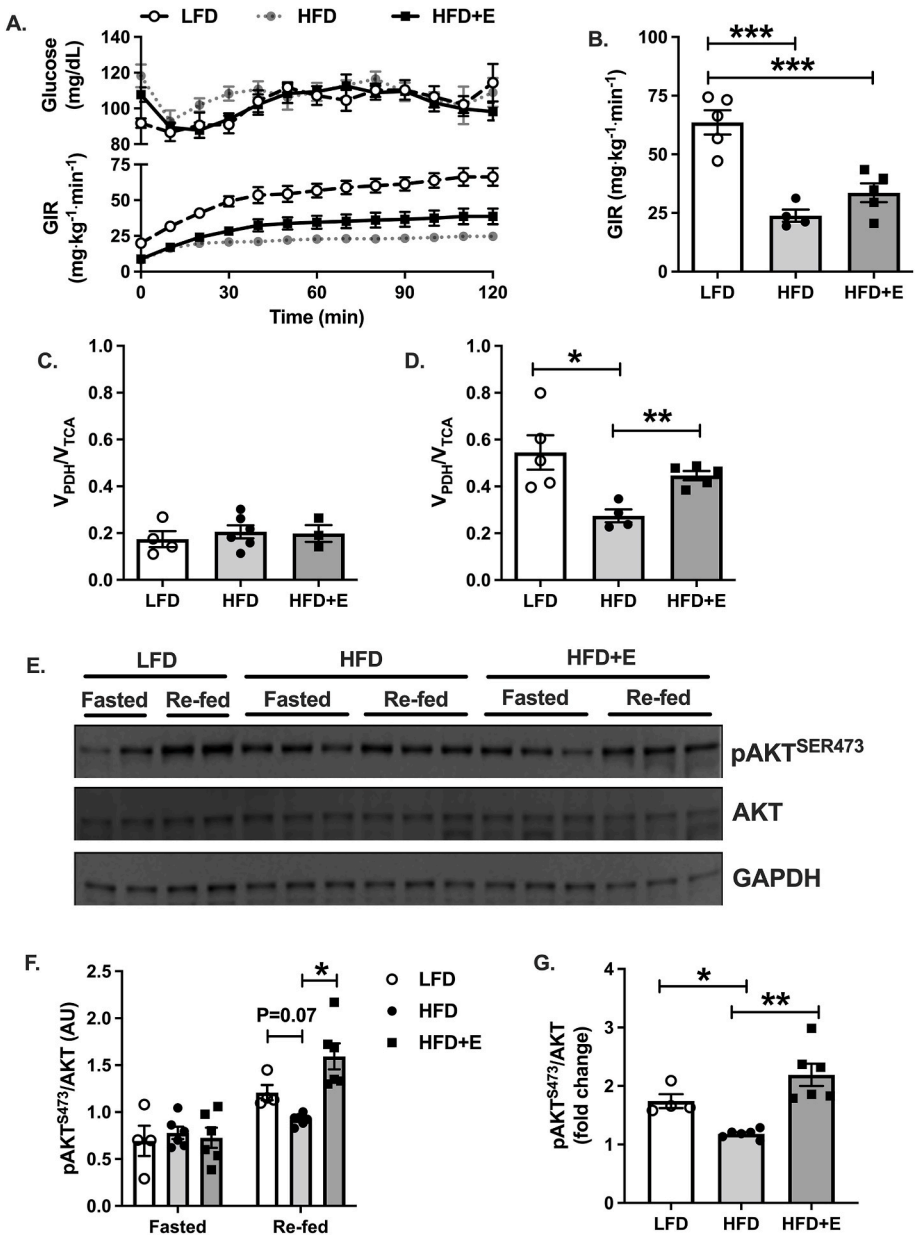

Fig. 3. EMPA restores cardiac metabolic flexibility. A. Time course data for plasma glucose levels and glucose infusion rates (GIR) during hyperinsulinemic euglycemic clamps. **B.** GIR at steady-state or final 40 min of the infusions shown in A. **C.** Relative glucose oxidation to fat oxidation or V_{PDH}/V_{TCA} measured in heart from fasted mice. **D.** V_{PDH}/V_{TCA} measured in heart following hyperinsulinemic euglycemic clamp. **E.** Representative immunoblots for phosphorylated AKT at serine 473 ($pAKT^{SER473}$), total AKT and GAPDH. **F.** Quantification of data in E. **G.** Fold-change in pAKT levels calculated from data in F. Data are the mean ± s.e.m. for groups of n = 4–6. Data were compared by one-way ANOVA and followed by multiple comparison testing to compare all groups when a significant effect was observed. *P < 0.05, **P < 0.01, ***P < 0.001.

hyperinsulinemia, V_{PDH}/V_{TCA} was significantly reduced in HFD compared with LFD and HFD + E mice, reflecting increased glucose utilization in LFD and HFD + E compared with HFD mice in response to insulin (Fig. 3D; $P < 0.05$ and $P < 0.01$, respectively). Insulin resistance plays an important role in obesity-associated metabolic inflexibility by reducing the amount of glucose transported and thus oxidized by cell types expressing the insulin-responsive glucose transporter GLUT4, such as skeletal and cardiac muscle (Galgani et al., 2008). To determine whether the observed differences in cardiac metabolic flexibility were associated with changes in insulin sensitivity in LFD and HFD + E compared with HFD mice, we measured changes in cardiac Akt phosphorylation. There were no differences in phospho-Akt during fasting (Fig. 3E&F); however, phospho-Akt was significantly increased in HFD + E compared with HFD mice, and there was a trend towards increased levels in LFD compared with HFD (Fig. 3E&F; $P < 0.05$ and $P = 0.07$, respectively). The fold-change in phospho-Akt in response to re-feeding was significantly reduced in HFD compared with LFD and HFD + E, demonstrating impaired insulin signaling in HFD mice that was reversed by EMPA (Fig. 3G; $P < 0.05$ and $P < 0.01$).

Metabolic flexibility and cardiac substrate selection are regulated by multiple factors including the expression and activity of key mediators of substrate selection, such as PDH and CPT1 (Fillmore et al., 2014). Phosphorylation of PDH, which leads to inhibition and reduced glucose oxidation, was similar between groups under fasted and re-fed conditions (Fig. 4A and B). Expression of *Cpt1b*, which facilitates mitochondrial fatty acid import and oxidation, was similar between groups in the fasted state, whereas in the re-fed state, *Cpt1b* expression was greater in HFD compared with LFD mice and there was no difference between HFD and HFD + E mice (Fig. 4C; $P < 0.05$). Expression of the glucose transporter *Glut4* was significantly different between groups in both the fasted and re-fed state, where *Glut4* expression was significantly less in HFD + E compared with LFD mice (Fig. 4D; $P < 0.05$), and levels tended to be reduced in HFD compared with LFD in the fasted state (Fig. 4D; $P = 0.07$). There were no differences in *Glut4* expression between HFD and HFD + E (Fig. 4D). Changes in *Glut1* expression followed a similar pattern as *Glut4* and were significantly reduced in HFD compared with LFD mice in the fasted state, whereas expression in HFD + E tended to be reduced, although not significantly (Fig. 4E; $P < 0.05$, $P < 0.07$).

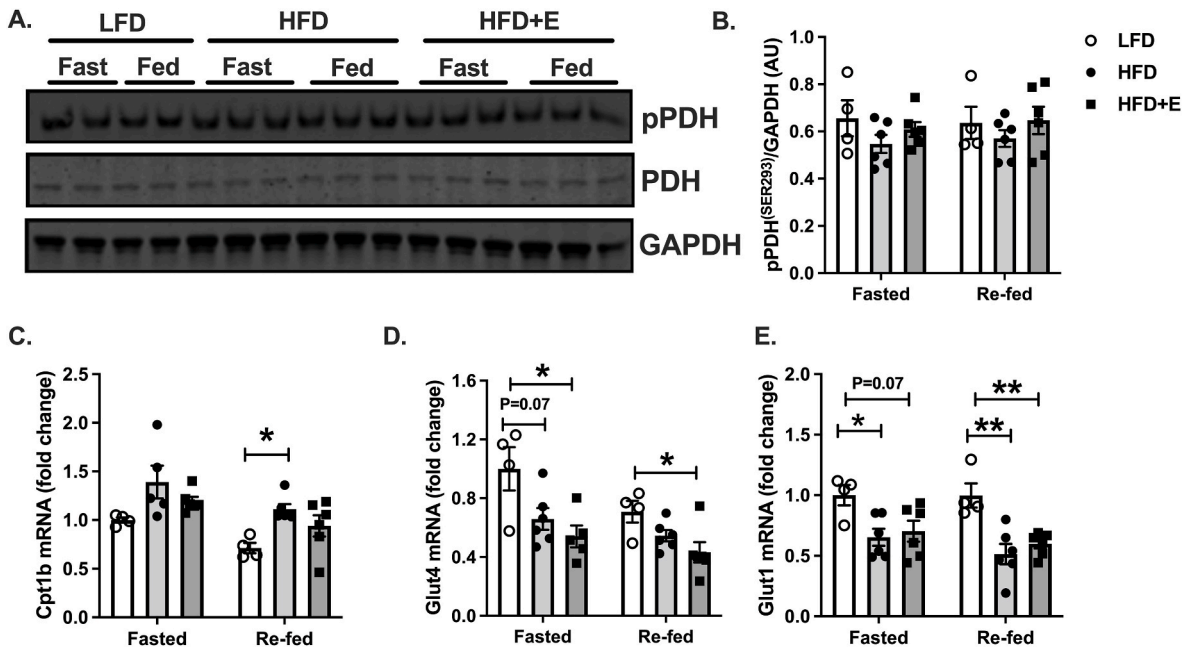

Fig. 4. Changes in PDH, CPT1 and autophagy do not account for changes in metabolic substrate utilization in EMPA-treated mice. A. Representative immunoblots for phosphorylated PDH at serine 293 (pPDHSER^{293}), total PDH and GAPDH. **B.** Quantification of data in A. **C-E.** Gene expression by QPCR. Data are the mean ± s.e.m. for groups of n = 4–6. Data were compared by one-way ANOVA and followed by multiple comparison testing to compare all groups when a significant effect was observed. *P < 0.05, **P < 0.01.

Following re-feeding, *Glut1* expression was significantly reduced in HFD and HFD + E compared with LFD mice (Fig. 4E; P < 0.01). There were no differences in *Glut1* expression between HFD and HFD + E mice in fasted or re-fed mice (Fig. 4E).

4. Discussion

In summary, we found that in the fasted state, relative rates of cardiac-specific glucose versus fatty acid utilization were similar in lean and diet-induced obese mice with or without EMPA treatment (Fig. 3C). The ability to increase glucose utilization in response to a physiological-stimuli, hyperinsulinemia, was impaired in the obese compared with lean mice and partially restored by EMPA treatment (Fig. 3D). Approximation of the fold change in relative glucose utilization in clamped versus fasted mice serves as an index of metabolic flexibility. LFD-fed mice displayed a 3.2-fold increase compared with 1.3- and 2.3-fold increases in HFD and HFD + E mice, demonstrating loss of cardiac-specific metabolic flexibility during obesity that was restored by EMPA. The improved cardiac glucose utilization and metabolic flexibility in EMPA-treated mice was associated with reduced cardiac hypertrophy (Fig. 2A&E), suggesting that the ability to use multiple metabolic substrates for energy production, particularly glucose, improved cardiac contractile efficiency and lessened compensatory hypertrophy. EMPA-treated mice were protected from ischemic stress (Fig. 2F&G), which may also result from their ability to increase glucose utilization in response to stress, thereby maximizing ATP production when oxygen levels are limiting and preventing cell death and subsequent adverse cardiac remodeling. Overall, our data support the notion that SGLT2 inhibitor therapy produces metabolic changes in heart that likely contribute to the CVD-protective effects of this class of drug.

While there is general agreement that the failing heart is bioenergetically compromised, in part due to altered metabolic substrate utilization where the heart favors metabolism of glucose over fatty acids (Neubauer, 2007; Neubauer et al., 1997), there is less agreement as to whether similar changes occur during diabetic cardiomyopathy prior to heart failure (Sowton et al., 2019). In general, studies performed *in vivo* using isotope tracing and preclinical animal models of insulin resistance demonstrated reduced cardiac glucose utilization and increased fatty acid utilization (Thapa et al., 2019; Mansor et al., 2013; Rohm et al., 2018; van den Brom et al., 2009; How et al., 2006) whereas studies performed *ex vivo* using models of insulin insufficiency detected reduced cardiac fatty acid utilization (Chatham and Forder, 1997; Chatham et al., 1999). Our data add to the growing body of *in vivo* evidence demonstrating that glucose metabolism is reduced and fatty acid metabolism is increased in models of diabetic cardiomyopathy, which likely results from cardiac insulin resistance, as well as increased plasma fatty acid levels that occur in these models. And although diabetic cardiomyopathy and heart failure differ from a metabolic standpoint in terms of substrate selection, both are characterized by the loss of metabolic flexibility or the use of the correct metabolic fuel given a specific physiological condition. Our data therefore suggest that the CVD-protective effects of EMPA may result in part from changes in cardiac metabolism and restored cardiac metabolic flexibility.

Indeed, a number of recent studies suggest that changes in cardiac metabolism contribute to the CVD-protective effects of EMPA therapy. In both diabetic and non-diabetic rodent studies, EMPA treatment resulted in improved cardiac mitochondrial function defined by increased *ex vivo* respiratory capacity and changes in gene expression suggesting increased mitochondrial biogenesis and increased utilization of both glucose and fatty acid metabolic substrates (Shao et al., 2019; Yurista et al., 2019). Our studies support and expand upon these observations by demonstrating *in vivo* changes in cardiac mitochondrial function following EMPA treatment, namely the ability to switch metabolic substrate utilization in response to changing physiological conditions, a feature of cardiac metabolism lost during diabetic cardiomyopathy and heart failure. Studies focused specifically on cardiac substrate utilization following EMPA treatment report somewhat different results. Using the *ex vivo* working heart system combined with isotope tracing, Verma and colleagues demonstrated that in a genetic model of obesity (*db/db*), EMPA increased cardiac glucose and fatty acid oxidation without affecting ketone use (Verma et al., 2018). In contrast, in a non-diabetic porcine model of heart failure, EMPA treatment reduced glucose utilization and partially restored fatty acid utilization, and ketone use was markedly enhanced (Santos-Gallego Carlos

Requena-Ibanez Juan Antonio San Antonio Rodolfo et al., 2019). Our studies differ from these in that we measured relative and not absolute rates of glucose and fatty acid utilization, and based on the design of our tracing strategy, we cannot discern the relative contribution of lipids, which includes fatty acids and ketones. So, while our studies clearly demonstrate that on a percent basis that glucose use during hyperinsulinemia is increased and lipid use, including fatty acids and ketones, is reduced in EMPA treated mice, they cannot address whether increases in the absolute amount of both glucose and lipid are increased, as reported *ex vivo* by Verma and colleagues, or whether absolute levels of ketone oxidation are increased in the absence of insulin, as reported by Santos-Gallego and colleagues. Despite challenges in comparing studies based on model systems and techniques used to assess changes in cardiac metabolism, a consistent observation across past studies and ours is that EMPA-treatment likely affects cardiac mitochondrial function and restores the bioenergetic capacity of the heart in both diabetic cardiomyopathy and heart failure (Verma et al., 2018; Shao et al., 2019; Yurista et al., 2019; Santos-Gallego Carlos Requena-Ibanez Juan Antonio San Antonio Rodolfo et al., 2019).

Despite the marked effects of EMPA on cardiac insulin sensitivity and glucose utilization in our studies, we did not observe significant effects on body weight or glucose homeostasis, which was somewhat of a surprise. SGLT2 inhibitor therapy has been shown to reduce body weight in several clinical trials (List et al., 2009; Wilding et al., 2009; Bailey et al., 2010; Neeland et al., 2016) and multiple studies employing rodent models of obesity, diabetes or CVD (Shao et al., 2019; Yurista et al., 2019; Xu et al., 2017; Katsuno et al., 2009). However, the effect on body weight in rodent studies appears to be dose and dose duration dependent. In low dose studies using 10 mg/kg, as was used in our studies, and dose durations of two to five weeks, changes in body weight were not observed, despite changes in heart metabolism and CVD endpoints, similar to what was observed herein (Verma et al., 2018; Habibi et al., 2017; N Dimitriadis et al., 2018; Han et al., 2008). In contrast, studies of longer duration (8–16 weeks) at 10 mg/kg, or longer duration and a higher dose of 30 mg/kg produced significant effects on body weight (Shao et al., 2019; Yurista et al., 2019; Katsuno et al., 2009). The mild to no of effect of EMPA on body weight and glucose homeostasis in our model therefore likely results from the low dose and short duration of dosing. Indeed, eight weeks of treatment of *db/db* mice with EMPA at the same dose used here improved insulin sensitivity (Kern et al., 2016).

Despite the mild phenotype observed with regards to glucose homeostasis, our studies did detect significant improvements in left ventricular mass in the HFD-fed EMPA-treated group. This reduced left ventricular hypertrophy is consistent with recent trials where both EMPA and dapagliflozin reduced left ventricular mass in patients with type 2 diabetes (Brown et al., 2020; Verma et al., 2019). In addition to improving left ventricular hypertrophy, EMPA has been shown to improve diastolic function (Santos-Gallego et al., 2021) potentially due to changes in cardiac bioenergetics during diastole (Garc í a-Ropero Á Vargas-Delgado et al., 2019). One of the limitations of our study with regards to the CVD phenotype reported is that we did not make any direct measures of diastolic function, nor did we measure changes in plasma markers of cardiac stress or cardiac infarct size or fibrosis after coronary artery ligation studies. Despite these limitations herein, several groups have reported reduced infarct size, myocardial cell death and susceptibility to cardiac arrhythmias in EMPA-treated rodents following ischemia/reperfusion injury (Hu et al., 2021; Andreadou et al., 2017; Lu et al., 2020).

Although our study cannot account for a single, mechanistic change by which EMPA restored cardiac metabolic flexibility, we observed a small number of changes in specific pathways that may contribute to the effect. First, cardiac-specific insulin sensitivity was improved by EMPA treatment (Fig. 3E–G), which would facilitate increased GLUT4-mediated glucose transport and thus glucose utilization. Second, systemic insulin sensitivity was mildly improved by EMPA (Fig. 3A and B) and the post-prandial suppression of adipose tissue lipolysis by insulin, calculated from the percent change in plasma fatty acid levels shown in Fig. 1E, was partially restored by EMPA; plasma fatty acid levels were reduced following re-feeding by 60% in LFD-fed mice compared with 25% in HFD and 40% in HFD + E mice. Thus, improved adipose tissue insulin sensitivity may have reduced fatty acid delivery to the heart and thus utilization in EMPA treated mice. Finally, we did not observe changes in PDH protein levels or phosphorylation, expression of *Cpt1β* or *Glut1/4* that could account for changes in substrate use, suggesting they did not contribute to the observed phenotype (Fig. 4A–E).

In conclusion, by using a novel approach to measure relative glucose versus fatty acid utilization in heart *in vivo*, we found that glucose utilization and metabolic flexibility are impaired in obese, insulin resistant mice compared with lean controls. More importantly, we found that SGLT2 inhibitor therapy restored insulin-stimulated glucose utilization and metabolic flexibility in heart, changes that were associated with reduced ventricular hypertrophy and protection from ischemic stress. These observations add to the growing list of potential mechanisms of action by which SGLT2 inhibitors are CVD-protective, and more broadly suggest that interventions that restore metabolic flexibility or glucose utilization in heart during diabetic cardiomyopathy may produce similar beneficial effects.

Grants

This work was supported by the Center for Metabolism and Mitochondrial Medicine (C3M) and funding provided by the Pittsburgh Foundation (MR 2020 109502), the University of Pittsburgh Rodent Ultrasonography Core through support from the NIH/OD S10 Instrumentation Program (OD023684), and the Health Sciences Metabolomics Core at the University of Pittsburgh and funding provided by the NIH (S10OD023402).

Disclosures

The authors declare that they have no competing interests.

CRediT authorship contribution statement

Bingxian Xie: Investigation, Validation, Formal analysis, Writing – original draft. **Wesley Ramirez:** Investigation, Validation, Writing – original draft. **Amanda M. Mills:** Investigation. **Brydie R. Huckestein:** Investigation, Validation. **Moira Anderson:** Investigation, Validation. **Martha M. Pangburn:** Investigation, Validation. **Eric Y. Lang:** Investigation, Validation. **Steven J. Mullet:** Investigation, Methodology. **Byron W. Chuan:** Investigation, Methodology. **Lanping Guo:** Investigation. **Ian Sipula:** Investigation, Formal analysis. **Christopher P. O'Donnell:** Resources, Methodology, Supervision. **Stacy G. Wendell:** Methodology, Supervision, Writing – original draft. **Iain Scott:** Conceptualization, Writing – review & editing, Supervision. **Michael J. Jurczak:** Conceptualization, Methodology, Formal analysis, Writing – review & editing, Visualization, Supervision, Funding acquisition.

Declaration of competing interest

The authors declare that they have no known competing financial interests or personal relationships that could have appeared to influence the work reported in this paper.

References

Alves, T.C., Befroy, D.E., Kibbey, R.G., Kahn, M., Codella, R., Carvalho, R.A., Falk Petersen, K., Shulman, G.I., 2011. Regulation of hepatic fat and glucose oxidation in rats with lipid-induced hepatic insulin resistance. Hepatology 53, 1175–1181.

Andreadou, I., Efentakis, P., Balafas, E., et al., 2017. Empagliflozin limits myocardial infarction in vivo and cell death in vitro: role of STAT3, mitochondria, and redox aspects. Front. Physiol. 8.

Anker, S.D., Butler, J., Filippatos, G., et al., 2021. Empagliflozin in heart failure with a preserved ejection fraction. N. Engl. J. Med. 385, 1451–1461.
Bailey, C.J., Gross, J.L., Pieters, A., Bastien, A., List, J.F., 2010. Effect of dapagliflozin in patients with type 2 diabetes who have inadequate glycaemic control with metformin: a randomised, double-blind, placebo-controlled trial. Lancet 375, 2223–2233.
Brown, A.J.M., Gandy, S., McCrimmon, R., Houston, J.G., Struthers, A.D., Lang, C.C., 2020. A randomized controlled trial of dapagliflozin on left ventricular hypertrophy in people with type two diabetes: the DAPA-LVH trial. Eur. Heart J. 41, 3421–3432.
Chatham, J.C., Forder, J.R., 1997. Relationship between cardiac function and substrate oxidation in hearts of diabetic rats. Am. J. Physiol. 273, H52–58.
Chatham, J.C., Gao, Z.P., Forder, J.R., 1999. Impact of 1 wk of diabetes on the regulation of myocardial carbohydrate and fatty acid oxidation. Am. J. Physiol. 277, E342–E351.
Edmunds, L.R., Xie, B., Mills, A.M., et al., 2020. Liver-specific Prkn knockout mice are more susceptible to diet-induced hepatic steatosis and insulin resistance. Mol. Metabol. 41, 101051.
Ferrannini, E., Muscelli, E., Frascerra, S., Baldi, S., Mari, A., Heise, T., Broedl, U.C., Woerle, H.-J., 2014. Metabolic response to sodium-glucose cotransporter 2 inhibition in type 2 diabetic patients. J. Clin. Invest. 124, 499–508.
Ferrannini, E., Baldi, S., Frascerra, S., Astiarraga, B., Heise, T., Bizzotto, R., Mari, A., Pieber, T.R., Muscelli, E., 2016a. Shift to fatty substrate utilization in response to sodium–glucose cotransporter 2 inhibition in subjects without diabetes and patients with type 2 diabetes. Diabetes 65, 1190–1195.
Ferrannini, E., Mark, M., Mayoux, E., 2016b. CV protection in the EMPA-REG OUTCOME trial: a "Thrifty substrate" hypothesis. Diabetes Care 39, 1108–1114.
Fillmore, N., Mori, J., Lopaschuk, G.D., 2014. Mitochondrial fatty acid oxidation alterations in heart failure, ischaemic heart disease and diabetic cardiomyopathy. Br. J. Pharmacol. 171, 2080–2090.
Galgani, J.E., Moro, C., Ravussin, E., 2008. Metabolic flexibility and insulin resistance. Am. J. Physiol. Endocrinol. Metab. 295, E1009–E1017.
García-Ropero Á, Vargas-Delgado, A.P., Santos-Gallego, C.G., Badimon, J.J., 2019. Inhibition of sodium glucose cotransporters improves cardiac performance. Int. J. Mol. Sci. 20, 3289.
Habibi, J., Aroor, A.R., Sowers, J.R., et al., 2017. Sodium glucose transporter 2 (SGLT2) inhibition with empagliflozin improves cardiac diastolic function in a female rodent model of diabetes. Cardiovasc. Diabetol. 16, 9.
Han, S., Hagan, D.L., Taylor, J.R., Xin, L., Meng, W., Biller, S.A., Wetterau, J.R., Washburn, W.N., Whaley, J.M., 2008. Dapagliflozin, a selective SGLT2 inhibitor, improves glucose homeostasis in normal and diabetic rats. Diabetes 57, 1723–1729.
How, O.-J., Aasum, E., Severson, D.L., Chan, W.Y.A., Essop, M.F., Larsen, T.S., 2006. Increased myocardial oxygen consumption reduces cardiac efficiency in diabetic mice. Diabetes 55, 466–473.
Hu, Z., Ju, F., Du, L., Abbott, G.W., 2021. Empagliflozin protects the heart against ischemia/reperfusion-induced sudden cardiac death. Cardiovasc. Diabetol. 20, 199.
Jia, Guanghong, Hill, Michael A., Sowers James, R., 2018. Diabetic cardiomyopathy. Circ. Res. 122, 624–638.
Katsuno, K., Fujimori, Y., Ishikawa-Takemura, Y., Isaji, M., 2009. Long-term treatment with sergliflozin etabonate improves disturbed glucose metabolism in KK-A(y) mice. Eur. J. Pharmacol. 618, 98–104.
Kern, M., Klöting, N., Mark, M., Mayoux, E., Klein, T., Blüher, M., 2016. The SGLT2 inhibitor empagliflozin improves insulin sensitivity in db/db mice both as monotherapy and in combination with linagliptin. Metabolism 65, 114–123.
Lam Carolyn, S.P., Chanchal, Chandramouli, Vineeta, Ahooja, Verma, Subodh, 2019. SGLT-2 inhibitors in heart failure: current management, unmet needs, and therapeutic prospects. J. Am. Heart Assoc. 8, e013389.
List, J.F., Woo, V., Morales, E., Tang, W., Fiedorek, F.T., 2009. Sodium-glucose cotransport inhibition with dapagliflozin in type 2 diabetes. Diabetes Care 32, 650–657.
Lopaschuk Gary, D., Verma, Subodh, 2020. Mechanisms of cardiovascular benefits of sodium glucose Co-transporter 2 (SGLT2) inhibitors. JACC: Basic Transl. Sci. 5, 632–644.
Lu, Q., Liu, J., Li, X., Sun, X., Zhang, J., Ren, D., Tong, N., Li, J., 2020. Empagliflozin attenuates ischemia and reperfusion injury through LKB1/AMPK signaling pathway. Mol. Cell. Endocrinol. 501, 110642.
Mansor, L.S., Gonzalez, E.R., Cole, M.A., Tyler, D.J., Beeson, J.H., Clarke, K., Carr, C.A., Heather, L.C., 2013. Cardiac metabolism in a new rat model of type 2 diabetes using high-fat diet with low dose streptozotocin. Cardiovasc. Diabetol. 12, 136.
McGaffin, K.R., Witham, W.G., Yester, K.A., Romano, L.C., O'Doherty, R.M., McTiernan, C.F., O'Donnell, C.P., 2011. Cardiac-specific leptin receptor deletion exacerbates ischaemic heart failure in mice. Cardiovasc. Res. 89, 60–71.
McMurray, J.J.V., Solomon, S.D., Inzucchi, S.E., et al., 2019. Dapagliflozin in patients with heart failure and reduced ejection fraction. N. Engl. J. Med. 381, 1995. –2008.
Neal, B., Perkovic, V., Mahaffey, K.W., de Zeeuw, D., Fulcher, G., Erondu, N., Shaw, W., Law, G., Desai, M., Matthews, D.R., 2017. Canagliflozin and cardiovascular and renal events in type 2 diabetes. N. Engl. J. Med. 377, 644–657.
Neeland, I.J., McGuire, D.K., Chilton, R., Crowe, S., Lund, S.S., Woerle, H.J., Broedl, U.C., Johansen, O.E., 2016. Empagliflozin reduces body weight and indices of adipose distribution in patients with type 2 diabetes mellitus. Diabetes Vasc. Dis. Res. 13, 119–126.
Neubauer, S., 2007. The failing heart — An engine out of fuel. N. Engl. J. Med. 356, 1140–1151.
Neubauer, S., Horn, M., Cramer, M., et al., 1997. Myocardial phosphocreatine-to-ATP ratio is a predictor of mortality in patients with dilated cardiomyopathy. Circulation 96, 2190–2196.
Packer, M., Anker, S.D., Butler, J., et al., 2020. Cardiovascular and renal outcomes with empagliflozin in heart failure. N. Engl. J. Med. 383, 1413–1424.
Perry, R.J., Shulman, G.I., 2020. Sodium-glucose cotransporter-2 inhibitors: understanding the mechanisms for therapeutic promise and persisting risks. J. Biol. Chem. 295, 14379–14390.
Rohm, M., Savic, D., Ball, V., Curtis, M.K., Bonham, S., Fischer, R., Legrave, N., MacRae, J.I., Tyler, D.J., Ashcroft, F.M., 2018. Cardiac dysfunction and metabolic inflexibility in a mouse model of diabetes without dyslipidemia. Diabetes 67, 1057–1067.
Santos-Gallego Carlos, G., Requena-Ibanez Juan Antonio, San Antonio Rodolfo, et al., 2019. Empagliflozin ameliorates adverse left ventricular remodeling in nondiabetic heart failure by enhancing myocardial energetics. J. Am. Coll. Cardiol. 73, 1931. –1944.
Santos-Gallego, C.G., Requena-Ibanez, J.A., San Antonio, R., et al., 2021. Empagliflozin ameliorates diastolic dysfunction and left ventricular fibrosis/stiffness in nondiabetic heart failure: a multimodality study. JACC Cardiovasc. Imag. 14, 393–407.
Shao, Q., Meng, L., Lee, S., Tse, G., Gong, M., Zhang, Z., Zhao, J., Zhao, Y., Li, G., Liu, T., 2019. Empagliflozin, a sodium glucose co-transporter-2 inhibitor, alleviates atrial remodeling and improves mitochondrial function in high-fat diet/streptozotocin-induced diabetic rats. Cardiovasc. Diabetol. 18, 165.
Shulman, G.I., Rossetti, L., Rothman, D.L., Blair, J.B., Smith, D., 1987. Quantitative analysis of glycogen repletion by nuclear magnetic resonance spectroscopy in the conscious rat. J. Clin. Invest. 80, 387–393.
Sowton, A.P., Griffin, J.L., Murray, A.J., 2019. Metabolic profiling of the diabetic heart: toward a richer picture. Front. Physiol. 10, 639.
Thapa, D., Xie, B., Zhang, M., et al., 2019. Adropin treatment restores cardiac glucose oxidation in pre-diabetic obese mice. J. Mol. Cell. Cardiol. 129, 174–178.
Vallon, V., Platt, K.A., Cunard, R., Schroth, J., Whaley, J., Thomson, S.C., Koepsell, H., Rieg, T., 2011. SGLT2 mediates glucose reabsorption in the early proximal tubule. J. Am. Soc. Nephrol. 22, 104–112.
van den Brom, C.E., Huisman, M.C., Vlasblom, R., et al., 2009. Altered myocardial substrate metabolism is associated with myocardial dysfunction in early diabetic cardiomyopathy in rats: studies using positron emission tomography. Cardiovasc. Diabetol. 8, 39.
Verma, Subodh, Rawat, Sonia, Ho Kim, L., et al., 2018. Empagliflozin increases cardiac energy production in diabetes. JACC: Basic Transl. Sci. 3, 575–587.
Verma, S., Mazer, C.D., Yan, A.T., et al., 2019. Effect of empagliflozin on left ventricular mass in patients with type 2 diabetes mellitus and coronary artery disease: the EMPA-HEART CardioLink-6 randomized clinical trial. Circulation 140, 1693–1702.
Voors, A.A., Angermann, C.E., Teerlink, J.R., et al., 2022. The SGLT2 inhibitor empagliflozin in patients hospitalized for acute heart failure: a multinational randomized trial. Nat. Med. 28, 568–574.
Wilding, J.P.H., Norwood, P., T'joen, C., Bastien, A., List, J.F., Fiedorek, F.T., 2009. A study of dapagliflozin in patients with type 2 diabetes receiving high doses of insulin plus insulin sensitizers: applicability of a novel insulin-independent treatment. Diabetes Care 32, 1656–1662.
Wiviott, S.D., Raz, I., Bonaca, M.P., et al., 2019. Dapagliflozin and cardiovascular outcomes in type 2 diabetes. N. Engl. J. Med. 380, 347–357.
Xu, L., Nagata, N., Nagashimada, M., Zhuge, F., Ni, Y., Chen, G., Mayoux, E., Kaneko, S., Ota, T., 2017. SGLT2 inhibition by empagliflozin promotes fat utilization and browning and attenuates inflammation and insulin resistance by polarizing M2 macrophages in diet-induced obese mice. EBioMedicine 20, 137–149.
Yurista, S.R., Silljé, H.H.W., Oberdorf-Maass, S.U., Schouten, E.-M., Pavez Giani, M.G., Hillebrands, J.-L., van Goor, H., van Veldhuisen, D.J., de Boer, R.A., Westenbrink, B. D., 2019. Sodium-glucose co-transporter 2 inhibition with empagliflozin improves cardiac function in non-diabetic rats with left ventricular dysfunction after myocardial infarction. Eur. J. Heart Fail. 21, 862–873.
Zinman, B., Wanner, C., Lachin, J.M., et al., 2015. Empagliflozin, cardiovascular outcomes, and mortality in type 2 diabetes. N. Engl. J. Med. 373, 2117–2128.
N, Nasiri-Ansari, Dimitriadis, G.K., Agrogiannis, G., Perrea, D., Kostakis, I.D., Kaltsas, G., Papavassiliou, A.G., Randeva, H.S., Kassi, E., 2018. Canagliflozin attenuates the progression of atherosclerosis and inflammation process in APOE knockout mice. Cardiovasc. Diabetol. 17, 106.